Glomerular Diseases

Research Article

Glomerular Dis 2023;3:197–210
DOI: 10.1159/000529700

Received: September 27, 2022
Accepted: February 4, 2023
Published online: August 20, 2023

Characterization of Membranous Nephropathy with Microspherular Deposits

Kevin Yi Mi Ren[a] Jean Hou[b]

[a]Department of Pathology and Molecular Medicine, Queen's University, Kingston, ON, Canada; [b]Department of Pathology and Laboratory Medicine, Cedars Sinai Medical Center, Los Angeles, CA, USA

Keywords
Microspherular · Microspherules · Membranous nephropathy · Electron microscopy

Abstract

Introduction: Membranous nephropathy (MN) is a common cause of adult nephrotic syndrome in the USA. The typical ultrastructural finding is of global uniformly dense subepithelial electron-dense immune complex deposits along glomerular basement membranes. However, early reports described deposits with a unique microspherular substructure. There was variability in what was identified as microspherular, sometimes overlapping with other entities such as podocyte infolding glomerulopathy. Currently, the nature, composition, and clinical significance of these microspherular deposits (MSDs) remain unknown. ***Method:*** We report the clinicopathologic features of a series of MN cases with MSD, with detailed ultrastructural characterization as well as PLA2R and THSD7A immunohistochemical and IgG subclass-staining characteristics. The proportion of MSD to overall deposits is segregated into two groups: global MSD with >50% MSD (n = 14) and segmental MSD with <50% (n = 5). ***Results:*** The size and appearance of the microspherules were nearly identical in global and segmental MSD groups (mean diameter of 77.9 nm and 77.2 nm, respectively), with subepithelial (n = 19) or intramembranous (n = 12) distributions in all cases. Mesangial MSDs (n = 5) were only found in the global MSD group. The majority of biopsies (86% of global MSD and 100% of segmental MSD) were Ehrenreich-Churg stage 2 or above; early stage 1 was only observed in the global MSD group. All but 3 cases were PLA2R/THSD7A double negative; 1 THSD7A positive in global MSD and 2 PLA2R positive in segmental MSD. IgG1 was the dominant subclass in the global MSD group, and IgG4 was dominant in the segmental MSD group, including the 2 PLA2R-positive cases. ***Conclusion:*** The findings suggest that MSDs are more commonly associated with secondary MN. This case series is the largest to date, and the findings may yield etiologic and prognostic information on this rare but unique subset of MN and provide a well-characterized cohort of cases for future studies.

Introduction

Membranous nephropathy (MN) has emerged as the most common cause of nephrotic syndrome in adults in the USA, surpassing focal and segmental glomerulosclerosis in most non-diabetic patient populations [1]. When MN is associated with a known secondary cause such as autoimmune diseases, malignancy, infections, or

karger@karger.com
www.karger.com/gdz

Correspondence to:
Jean Hou, Jean.Hou@CSHS.org

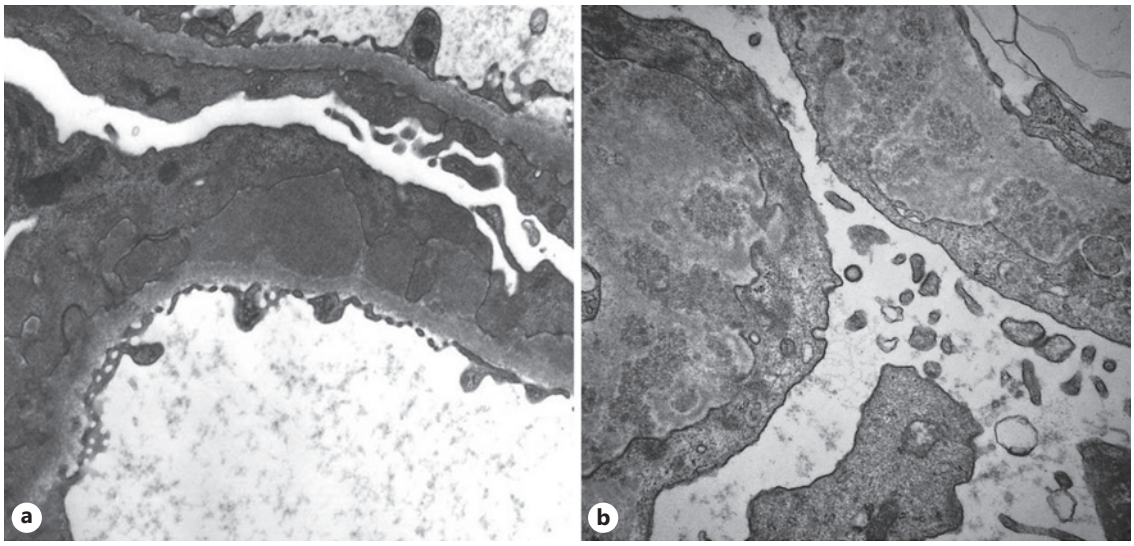

Fig. 1. Differing ultrastructural appearances observed in membranous nephropathy. **a** Electron microscopy findings of a case of MN with conventional amorphous and finely granular subepithelial electron-dense deposits separated by intervening spikes of basement membrane material. Subepithelial deposits with microspherular substructure are shown in panel **b**, in the same pattern and distribution as the typical subepithelial deposits shown in panel **a**. ×14,000 magnification.

medications, it has been considered "secondary." In contrast, cases of MN without a recognizable secondary cause were once considered "primary" or "idiopathic." The separation of MN into "primary" and "secondary" was primarily based on treatment implications as a diagnosis of secondary MN would prompt an infectious, autoimmune, and malignancy workup.

Idiopathic MN had been theorized to be an autoimmune disease. However, the breakthrough discovery of the first target antigen on podocytes, phospholipase A2 receptor 1 (PLA2R) in approximately 70% of idiopathic MN cases completely shifted the paradigm in how MN is diagnosed and monitored [2, 3]. A second podocyte antigen, thrombospondin type-1 domain-containing 7A (THSD7A), was later discovered to account for another 3–5% of primary MN. The last decade has seen rapid-fire discovery of additional target antigens: exostosin 1(EXT1)/exostosin 2(EXT2), most commonly associated with autoimmune diseases [4]; semaphorin 3B, more common in pediatric patients [4]; NELL1 (along with THSD7A), more often associated with malignancy [5]; and most recently netrin G, another podocyte antigen [6]. The observation that different target antigens MN positivity can coexist (possibly coincidentally) with "secondary" diseases, and that distinct clinical phenotypes are associated with different target antigens have supported proposals to reclassify MN in terms of target antigens and associated diseases rather than primary or secondary, to promote more effective treatment strategies [7].

The histologic diagnosis of MN is defined by subepithelial immune complex deposits along glomerular basement membranes (GBMs) with global or segmental GBM involvement. Segmental subepithelial deposits and concomitant subendothelial or mesangial glomerular deposits may favor secondary over idiopathic MN. The subepithelial deposits typically display a uniformly amorphous or finely granular electron-dense texture by electron microscopy (EM) (shown in Fig. 1) [8]. However, reports of MN cases with deposits composed of a unique microspherular substructure have been described for decades, with the largest series of 14 cases reported by Kowalewska et al. [9] in 2006 and the most recent case series by Choung et al. [10] in 2022.

The microspherular substructures have been hypothesized to represent nuclear pore or viral particles [11, 12]. In addition, many reports from Japan have described cases with atypical EM findings of microspherular and/or microtubular substructures associated with podocyte infolding into the GBM or podocyte infolding glomerulopathy (PIG) [13–15]. However, Kowalewska et al. [9] demonstrated that the microspherular deposits (MSDs) did not stain with antibodies against nuclear pore components or podocyte protein CD10. As yet, the nature

and composition of these MSD remain unknown. While case reports of PIG have described some atypical deposits as microspherular, the images have demonstrated a considerable range in appearance from discrete spherules to microtubules, sometimes with interdigitating connections with overlying podocytes seen in PIG [13]. The light microscopy (LM) diagnosis in PIG is also heterogeneous and not limited to MN [13]. In order to differentiate true MSD from other entities, we characterized the MSD by detailed ultrastructural, immunofluorescence (IF), and immunohistochemical (IHC) evaluation and attempt to uncover relevant clinical and diagnostic correlations.

Materials and Methods

Institutional Ethics Review approval was obtained (STUDY00001348). All kidney biopsies accessioned in the Department of Pathology at Cedars-Sinai Medical Center from 2005 to 2019 were queried for diagnoses of MN and any of the following descriptive words for glomerular deposits: "nuclear pore"; "microspherule"; "microsphere"; "microspherular"; "spherule"; "sphere"; or "spherular." A total of 26 cases were identified. Archived digitized electron micrographs were reviewed, and ultrastructural studies repeated on all 26 cases to examine the location, distribution, and size of the MSD. Following detailed analysis, 19 of the 26 cases were determined to contain MSD which appeared ultrastructurally uniform and consistent. Seven cases with deposits displaying deviant substructure/organization were excluded from further analysis. Of the 19 included cases, there were 17 native (including 2 biopsies from the same patient performed 4 years apart) and 2 allograft biopsies. Digitized photomicrographs of LM were reviewed, and when available, glass slides were re-evaluated to examine and document pertinent glomerular histologic features (segmental sclerosis, crescents/necrosis, endocapillary hypercellularity, and mesangial hypercellularity). Staining for PLA2R and THSD7A was performed, if not done previously. A routine IF panel and IgG subclass staining was performed for all obtainable cases.

Demographic, clinical, and laboratory data at the time of biopsy for each patient were reviewed and recorded when available. Elevated serum creatinine is defined as greater than 1.25 mg/dL (110.5 μmol/L) [16]. Nephrotic range proteinuria is defined as 24-h urinary protein excretion more than 3.5 g/24 h. Nephrotic syndrome is defined by the combination of nephrotic range proteinuria, hypoalbuminemia (serum albumin less than 3 g/dL), and peripheral edema. Comorbidities identified in the past medical history (e.g., hypertension, diabetes, autoimmune disease, infection, malignancy, etc.) were also recorded.

Light Microscopy

All renal biopsies were processed using standard techniques for LM, IF, and EM at Cedars-Sinai Medical Center. Tissue for LM was fixed in either alcoholic Bouin's fixative (native biopsy) or 10% buffered formalin (allograft biopsies) and paraffin-embedded (with hematoxylin-eosin, periodic acid-Schiff, Masson's trichrome, and Jones silver methenamine stains of 2-micron-thick sections).

Immunohistochemistry

Monoclonal antibody against human PLA2R (CL0474) and polyclonal antibody to human THSD7A were obtained from Sigma (St. Louis, MO, USA). IHC was performed at 1:500 dilution for both antibodies on unstained 2-micron thick sections from alcoholic Bouin's solution or formalinfixed paraffin-embedded tissue for PLA2R and formalin-fixed frozen tissue sections for THSD7A.

Immunofluorescence

Renal biopsy tissue collected in Zeus solution was snap-frozen for direct IF with fluoresceinated antisera to human IgG, IgA, IgM, C3, C1q, albumin, fibrin, κ and λ light chains, as well as direct IF for human IgG subclass (IgG1, IgG2, IgG3, and IgG4).

Electron Microscopy

A portion of cortical tissue was also fixed in 4% glutaraldehyde for EM, and ultrathin sections of plastic-embedded tissue were cut, stained with uranyl acetate and lead citrate, and examined in a JEOL JEM-1010 or 100CX transmission electron microscope (JEOL Ltd., Tokyo, Japan). All available open glomeruli on the EM grid for each case (between 1 and 5 glomeruli) were examined. The diameter of MSD was measured at ×72,000 magnification and between 7 and 90 measurements were taken for each case.

Results

Electron Microscopy

Detailed ultrastructural examination was performed on all 19 cases and the findings are summarized in Table 1. All cases had variably irregular GBM contours and numerous subepithelial and/or incorporated intramembranous deposits not only with typical homogenous or granular electron densities but also with at least focal MSD composed of discrete or clusters of microspherules with an average diameter of 77.8 nm (range 37.3 nm–153 nm; SD 15.2 nm). Some MSD had a circular appearance with an electron-dense periphery and relatively electron-lucent core. The distribution of MSD with respect to the GBM varied. Most cases had subepithelial MSD which were either separated by intervening spikes of GBM material (Ehrenreich and Churg stage 2) (shown in Fig. 2a) [17] or were incorporated/intramembranous and associated with a "neomembrane" between deposits and podocytes (stage 3) (shown in Fig. 2b). Fewer MSD formed superficial indentations on the external surface of the GBMs without "spike" formation (Ehrenreich and Churg stage 1) or were primarily resorbed (stage 4).

Cases were separated into two groups based on the proportion of all GBM deposits containing MSD. 14 of 19 cases had more than 50% MSD (global MSD) and 5 cases

Table 1. Electron microscopy distribution and characteristics of microspherular deposits (MSDs) in MN

	Global MSD	Segmental MSD
	14 cases (13 patients)	5 cases (5 patients)
Ehrenreich and Churg stage (predominant), *n* (%)		
1	2 (14)	0 (0)
2	2 (14)	3 (60)
3	7 (50)	0 (0)
4	3 (22)	2 (40)
Location of MSD, *n* (%)		
Subepithelial	14 (100)	5 (100)
Subendothelial	0 (0)	0 (0)
Intramembranous	10 (77)	2 (40)
Mesangial*	5 (38)	0 (0)
Extraglomerular	0 (0)	0 (0)
% of deposits that are MSD, *n* (%)		
>95%	10 (71)	0 (0)
75–95%	3 (21)	0 (0)
50–74%	1 (7)	0 (0)
<50%	0 (0)	5 (100)
MSD diameter (mean)	77.9 nm	77.2 nm
Striated membranous structures, *n* (%)	14 (100)	5 (100)

*Cases with mesangial deposits also have intramembranous deposits.

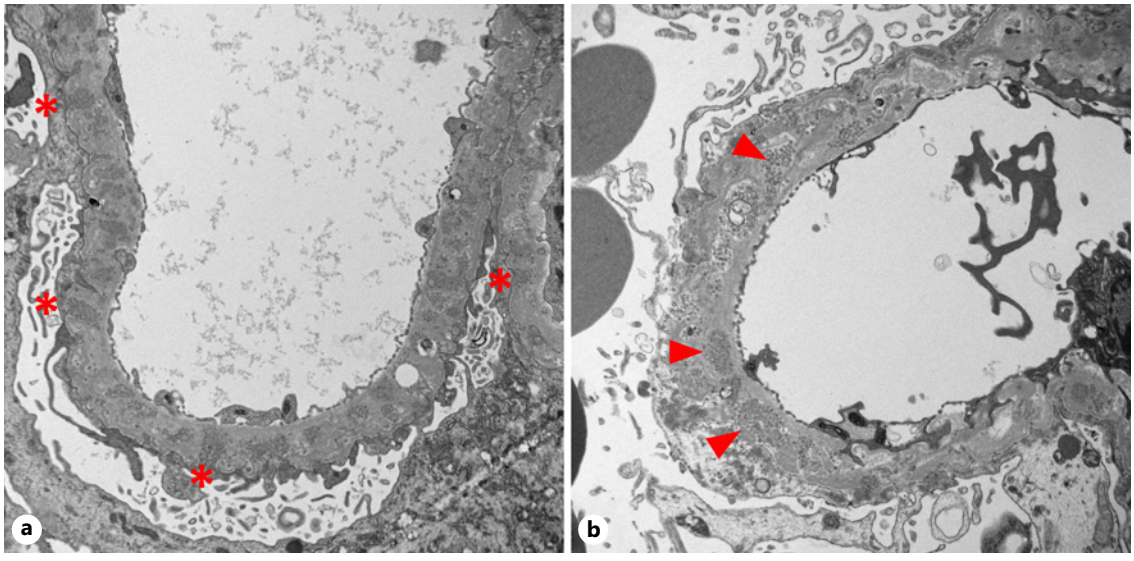

Fig. 2. Ultrastructural appearance and distribution of MSD appear similar in representative cases from global MSD (**a**) and segmental MSD (**b**). Electron microscopy reveals characteristic microspherular substructure that can appear in various stages, ranging from Ehrenreich and Churg stage 2 (**a**, asterisks) where deposits are separated by intervening spikes of basement membrane material, to stage 3 (**b**, arrowheads) where the deposits have been incorporated within the GBMs and are associated with the formation of a neomembrane between the deposits and overlying podocytes. ×7,200 magnification.

had MSD comprising less than 50% (segmental MSD). The non-MSD deposits were of the usual uniformly electron-dense immune complex type. All cases contain non-specific striated membranous structures that may represent degradation products from cellular components [18]. No other organized substructure deposits

(including fingerprint, fibrillar, and microtubular substructures) were identified. In the global MSD group, the MSDs were quite extensive and comprised more than 95% of all GBM deposits in 10 cases and at least 75% in another 3 cases. Only 1 case contained less than 75% MSD, diagnosed as membranous lupus nephritis (LN). The MSDs in the global MSD group were identified predominantly in GBMs: subepithelial (n = 14) and intramembranous (n = 10). However, 5 cases had concomitant mesangial MSD, suggestive of a secondary etiology. No subendothelial MSDs were present. The MSD had an average diameter of 77.9 nm (range 37.3 nm–133 nm; SD 14.3 nm). Interestingly, the other 2 membranous LN cases in the global MSD group displayed a mixture of deposits, with typical granular electron-dense deposits in the mesangium but MSD in GBMs. Two biopsies were from the same patient performed 4 years apart; both biopsies had global MSD. One biopsy from a patient with membranous LN and global MSD had a previous biopsy 11 years prior that showed advanced membranous LN without any evidence of MSD. All cases showed extensive podocyte foot process effacement without evidence of infolding. No extraglomerular MSD were identified. Tubuloreticular inclusions were found only in 1 case of LN.

In the segmental MSD group, the MSD comprised less than 10% of all deposits in 4 of the 5 cases and less than 20% in one. All segmental MSD were subepithelial (n = 5); 2 cases also had intramembranous MSD. None had subendothelial or mesangial MSD. The microspherular substructures were morphologically similar to those seen in the global MSD group, with an average diameter of 77.2 nm (range 44.3 nm–153 nm; SD 19.0 nm). All cases also showed extensive podocyte foot process effacement. No typical or MSD extraglomerular deposits or tubuloreticular inclusions were identified.

Clinical Information

Clinical and pathological data from global and segmental MSD cases are summarized in Tables 2 and 3, respectively. In the global MSD group, there were 5 (38%) men and 8 (62%) women. The mean age at the time of biopsy was 56 years (range, 33–88 years). All patients had some degree of proteinuria. More than half (6) had nephrotic range proteinuria, 3 of whom had nephrotic syndrome. Four patients had hematuria, and 3 had elevated serum creatinine. Concurrent medical conditions with potential renal implications included hypertension in 5 patients, diabetes in 2, systemic lupus erythematosus (SLE) in 3, and hepatitis C virus (HCV) infection in 1. One patient had positive serum ANA without an established diagnosis of autoimmune disease.

In the segmental MSD group, there were 2 men and 3 women. The mean age at the time of biopsy was 53 years (range, 25–68 years). All patients had proteinuria; 3 with nephrotic syndrome. No patients had concurrent hematuria, and 4 had elevated serum creatinine. Concurrent medical conditions with potential renal implications included hypertension in 1 patient, and diabetes and systemic lupus in 1 other. Four biopsies were from native kidneys, and 1 biopsy was from a transplant.

Light Microscopy

The LM findings are summarized in Table 4. In the global MSD group, one (1) case had medulla only and no glomeruli for LM examination; the remaining 13 cases had between 4 and 61 patent glomeruli. Nine of the 13 cases had at least one glomerulus with segmental sclerosis. LM features for global and segmental MSD were similar. All cases had diffuse GBM irregularities in contour with variable intramembranous lucencies and/or subepithelial spikes by silver stain (shown in Fig. 3) and fuchsinophilic subepithelial deposits by trichrome stain. Two (2) native biopsies had segmental GBM double contours, and the single allograft biopsy had diffuse GBM double contours consistent with transplant glomerulopathy. One native biopsy contained fibrin thrombi with intracapillary leukocytes, but none had true endocapillary hypercellularity, crescents, or necrosis. Three cases had no significant interstitial fibrosis and tubular atrophy (IF/TA); 9 had mild and 1 had moderate IF/TA. One native biopsy had acute tubulointerstitial nephritis. Six cases had acute tubular injury. Arteriosclerosis and arteriolosclerosis were present in 10 and 7 cases, respectively. Thrombotic microangiopathic or vasculitic features were not observed in any cases.

In the segmental MSD group, all cases had at least one glomerulus with segmental sclerosis. One case had segmental GBM double contours. No endocapillary hypercellularity, crescents, or necrosis were identified in any cases. Four cases had mild and 1 had moderate IF/TA. Two biopsies had acute tubulointerstitial nephritis, and 4 cases had acute tubular injury. Arteriosclerosis and arteriolosclerosis were present in 2 and 4 cases, respectively. Thrombotic microangiopathic or vasculitic features were not observed in any cases.

Immunohistochemistry for PLA2R and THSD7A

The IHC findings are summarized in Table 4. In the global MSD group, all 12 cases with available tissue were negative for PLA2R (shown in Fig. 4). Only 1 case was

Glomerular Dis 2023;3:197–210
DOI: 10.1159/000529700

Table 2. Clinical and pathologic features of MN with global microspherular deposits (MSDs)

Patient No.	Age, years/ gender	Clinical presentation	Concurrent disease	Renal pathology diagnosis	Extent of MSD, %	Location of MSD	Stage	PLA2R	THSD7A	Capillary IgG	Dominant IgG subclass	Mesangial staining	Extraglomerular deposits
1	45/M	Proteinuria	N/A	MN	>80	Subepi, intramemb	3	N/A[#]	N/A[#]	N/A*	N/A*	N/A*	No
2	75/F	Proteinuria, hematuria, elevated creatinine	+ANA	MN	>90	Subepi	2	Negative	Negative	2–3+ granular	IgG1, 2+	IgM, 1–2+	No
3	46/M	Nephrotic syndrome, hematuria	HTN	MN	100	Subepi, intramemb	2	Negative	Negative	2–3+ granular	IgG1, 2+	IgM, 1–2+	No
4 (Biopsy1)	61/F	Nephrotic syndrome, hematuria	HTN Neg serology	MN	100	Subepi	1	Negative	Negative	Trace-1+ granular	IgG1, trace-1+	IgM, trace-1+	No
4 (Biopsy2)	66/F	Recurrent proteinuria with known MN	HTN Neg serology	Inactive MN	>80	Subepi, intramemb	4	Negative	Negative	Trace granular	IgG1, trace	No	No
5 Allograft	58/M	Proteinuria, elevated creatinine	HCV	MN	>90	Subepi, intramemb, mes (occasional)	4	Negative	Negative	Trace granular	IgG1, 0-trace	No	No
6	43/F	Recurrent proteinuria with known MN	N/A Neg serology	Advanced MN	100	Subepi, intramemb, mes (frequent)	3	Negative	Negative	3+ granular	IgG1, 3+	No	No
7	57/F	Proteinuria	N/A	MN	100	Subepi, intramemb, mes (occasional)	3	Negative	Negative	2+ granular	IgG1, 1+	No	No
8	88/F	Nephrotic range proteinuria	HTN, hypothyroidism Neg serology	MN	100%	Subepi, intramemb	3	Negative	Negative	3+ granular	IgG1, 3+	No	No
9	61/M	Progressive proteinuria	HTN, dyslipidemia neg serology	MN	100	Subepi, intramemb	3	Negative	Negative	3+ granular	IgG1, 2–3+	IgA, 2+, segmental	No
10	58/M	Proteinuria	HTN, diabetes, dyslipidemia neg serology	MN	100	Subepi, intramemb, mes (occasional)	3	Negative	Positive	2–3+ granular	IgG1, 2–3+	IgG, 1+, segmental IgA, 1+ C3, 1+	No
11	41/F	Heavy proteinuria, hematuria	SLE	Membranous LN, ISN/RPS Class 5	50–60	Subepi	3	Negative	Negative	1+ granular	IgG1, 2+	IgG, 2–3+ IgM, trace C1q, 2–3+ C3, 1–2+	TBM
12	47/F	Nephrotic syndrome	SLE	MN, consistent with membranous LN ISN/RPS class 5	100	Subepi, intramemb, mes (occasional)	4	Negative	Negative	3–4+ granular	IgG1, 2–3+	IgG, 2–3+ IgM, 1+ C1q, trace to 1+	No
13	33/F	Sub-nephrotic proteinuria hypocomplementemia	SLE	MN, consistent with membranous LN ISN/RPS class 5	100	Subepi, intramemb	1	Negative	Negative	N/A*	N/A*	N/A*	No

MSDs, microspherular deposits; N/A, not available; subepi, subepithelial; intramemb, intramembranous; ANA, anti-nuclear antibody; HTN, hypertension; neg, negative; MN, membranous nephropathy; HCV, hepatitis C virus; mes, mesangial; SLE, systemic lupus erythematosus; LN, lupus nephritis; ISN/RPS, International Society of Nephrology/Renal Pathology Society; TBM, tubular basement membrane. [#]No glomeruli available for immunohistochemistry. *No glomeruli available for IF.

positive for THSD7A (not shown), and no underlying malignancy was identified in this patient. In the segmental MSD group, 4 of 5 cases had tissue available for IHC, of which 2 showed positive staining for PLA2R and none showed positive staining for THSD7A (shown in Fig. 5).

Immunofluorescence

Standard IF panel consisting of IgG, IgA, IgM, C1q, C3, albumin, fibrinogen, and κ and λ light chains was performed in 12 global MSD and all 5 segmental MSD cases. The IF findings are summarized in Tables 2 and 3. In the global MSD group, all 12 cases showed at least trace granular IgG staining along GBMs; 8 with at least 2+ staining intensity. Three cases also had ≥ trace granular IgA co-staining along GBMs; 2 in membranous LN. One case had 1+ granular IgM co-staining in GBMs and another had segmental irregular coarse granular staining for IgM in a distribution distinct from IgG. Only 2 cases had positive staining for C1q in the mesangium, both from patients with SLE and membranous LN. Ten (10) cases had ≥ trace granular staining for C3 along GBMs, two also with ≥1+ granular mesangial C3 staining. Staining for κ and λ light chains had approximately equivalent intensity with a similar distribution as IgG and C3. Three cases showed concomitant mesangial deposits which stained ≥1+ granular staining for IgG and 3 other cases had ≥ trace granular mesangial IgM staining. One case had 2+ granular mesangial IgA staining without corresponding mesangial MSD and may represent low-grade IgA nephropathy.

In the segmental MSD group, 4 of the 5 cases showed ≥ trace granular IgG staining along GBMs; 3 cases had ≥3+ IgG. The single IgG-negative case had trace to 1+ granular C3 only staining in GBMs which corresponded with resolving typical intramembranous deposits by EM and was interpreted as moderately advanced MN. Although this patient had SLE, the findings were not consistent with membranous LN. One case showed segmental trace granular staining for IgA and C1q along GBMs, insufficient to diagnose membranous LN but was PLA2R positive. All 5 segmental MSD cases showed ≥ trace granular C3 along GBMs. Staining for κ and λ light chains had approximately equivalent intensity and had similar distribution as IgG and C3. 4 cases had ≥ trace concomitant granular mesangial IgM staining.

IgG Subclass IF

IF IgG subclass panel (IgG1, IgG2, IgG3, and IgG4) was also performed on 12 cases in the global MSD group and 4 cases in the segmental MSD group. All 12 global MSD cases had ≥ trace granular IgG1 staining along GBMs; 7 had ≥2+ IgG1 staining. Eight cases were IgG2 negative, and the 4 IgG2-positive cases displayed at most trace to 1+ intensity. Seven cases had IgG3 staining along GBMs, 6 of which were ≤1+. Three cases were IgG4 positive, all with trace intensity. Overall, IgG1 represented the dominant IgG subclass in all 12 global MSD cases (shown in Fig. 4).

In the segmental MSD group, all 4 available cases showed ≥ trace granular IgG1 staining along GBMs; 3 also showed strong and dominant (≥3+) staining for IgG4, with variable lesser intensity staining for IgG2 and IgG3. One case was negative for IgG and all IgG subclasses. Overall, 3 cases were IgG4 dominant and one was IgG1 dominant (shown in Fig. 5).

Discussion

We report our institutional experience with a series of MN cases containing MSD deposits. Glomerular deposits with microspherular substructure have been described for decades [9–11, 19–24]. However, the reports seemed somewhat inconsistent in the definition of the term, microspherular, and there was some descriptive overlap with PIG, which has quite distinctive ultrastructural features. Even recently, one case report describing a patient with PIG showed deposits nearly identical in size and ultrastructural appearance to MSDs [25]. With access to a vast archive of kidney biopsies, we sought to define and characterize these MSDs and investigate the clinical and potential diagnostic significance of this intriguing entity.

In our cohort, initial ultrastructural evaluation broadly divided the cases into 2 groups, global MSD and segmental MSD based on whether MSD made up greater or less than 50% of all GBM deposits. However, the actual proportion of MSD in all deposits displayed a sizeable gap, segregating to either extreme: ≤20% in segmental MSD and ≥75% in global MSD. The ultrastructural appearance of the MSD were consistent for both global and segmental MSD, with scattered or clusters of microspherules measuring between 77 and 78 in average diameter, supporting a common composition but in distinct distributions and possibly differing pathogenesis.

MSDs were not limited to the GBMs; in 5 of the 12 patients, global MSD in GBMs were accompanied by mesangial deposits, 4 of which were MSD. These findings support a single pathogenic mechanism for both GBM and mesangial deposits, and the coexistence in both glomerular locations is also suggestive of a secondary

Glomerular Dis 2023;3:197–210
DOI: 10.1159/000529700

Table 3. Clinical and pathologic features of MN with segmental microspherular deposits (MSDs)

Patient No.	Age, years/ gender	Clinical presentation	Concurrent disease	Renal pathology diagnosis	Extent of MSD, %	Location of MSD	Stage	PLA2R	THSD7A	Capillary IgG	Dominant IgG subclass	Mesangial staining	Extraglomerular deposits
14	25/F	Worsening renal graft function and proteinuria	ESRD from hypoplastic kidney 17 y.o graft De novo MN 3 years post transplantation	Resolving MN	5–10	Subepi, intramemb	4	Negative	Negative	Trace-1+	IgG1, trace	No	No
15	66/M	Nephrotic syndrome elevated creatinine	N/A	MN	5	Subepi	2	Positive	Negative	4+	IgG4, 4+	IgM, 1+	No
16	48/F	Elevated creatinine	Systemic lupus (no LN on previous biopsy 5 years prior) diabetes	MN	10–20	Subepi, intramemb	4	Negative	Negative	None	None	IgM, trace, segmental	No
17	56/F	Nephrotic syndrome	N/A	MN	10	Subepi	2	N/A (block missing)	N/A	4+	IgG4, 4+	IgM, 2+	No
18	68/M	Nephrotic syndrome elevated creatinine	Hyperlipidemia neg serology	MN	<5	Subepi	2	Positive	Negative	3–4+	IgG4, 3–4+	IgM, trace	No

MSDs, microspherular deposits; ESRD, end-stage renal disease; MN, membranous nephropathy; subepi, subepithelial; intramemb, intramembranous; N/A, not available; neg, negative.

Table 4. Light microscopy (LM) findings in MN with MSDs

	Global MSD	Segmental MSD
	13 cases (12 patients)*	5 cases (5 patients)**
Glomerular, *n* (%)		
Segmental sclerosis	9 (69)	5 (100)
Crescents/fibrinoid necrosis	0 (0)	0 (0)
Endocapillary hypercellularity	0 (0)	0 (0)
Mesangial hypercellularity	2 (15) (segmental)	0 (0)
Tubulointerstitial inflammation, *n* (%)	3 (23)	2 (40)
Interstitial fibrosis/tubular atrophy, *n* (%)		
None	3 (23)	0 (0)
Mild	9 (69)	4 (80)
Moderate	1 (8)	1 (20)
Severe	0 (0)	0 (0)
Acute tubular injury, *n* (%)	6 (46)	4 (80)
Arteriosclerosis, *n* (%)	10 (77)	2 (40)
Arteriolosclerosis, *n* (%)	7 (54)	4 (80)
PLA2R,** *n* (%)	0 (0)	2 (40)**
THSD7A,** *n* (%)	1 (8)	0 (0)**

Mild <25% IF/TA, moderate 25–50% IF/TA, severe >50% IF/TA. *One case inadequate for LM. **One case inadequate for IHC.

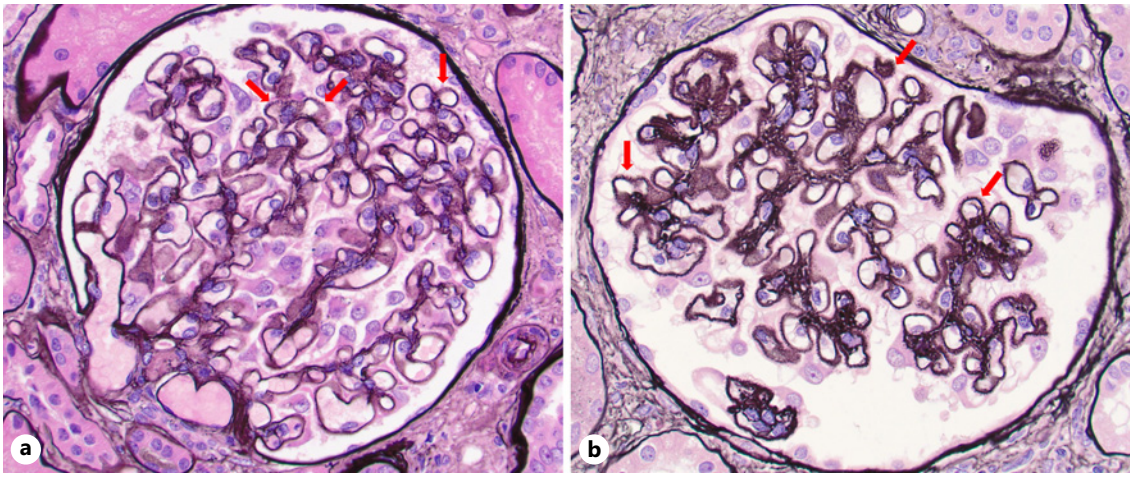

Fig. 3. Light microscopic findings from cases from global MSD (**a**) and segmental MSD (**b**) groups are similar and do not predict proportion of MSD in overall subepithelial deposits. Subepithelial spikes can appear early (**a**, arrows) to more prominent (**b**, arrows). Jones methenamine silver, ×400 magnification.

etiology [26]. Clinically, 4 of 12 global MSD patients had documented potential secondary causes: 3 SLE patients with membranous LN and 1 patient with HCV infection. One other patient had positive ANA but without a diagnosis of autoimmune disease. Only one of the 3 membranous LN cases had MSD in both GBMs and mesangium; the remaining 2 had typical, non-MSD mesangial deposits. Interestingly, GBM and mesangial MSDs corresponded with stronger IgG staining, while the cases with typical mesangial deposits had stronger C1q staining. In both mixed deposit cases, IgG1 was the dominant IgG subclass in the capillary wall deposits, while IgG3 was the dominant or codominant IgG subclass in the mesangial deposits. These findings suggest the

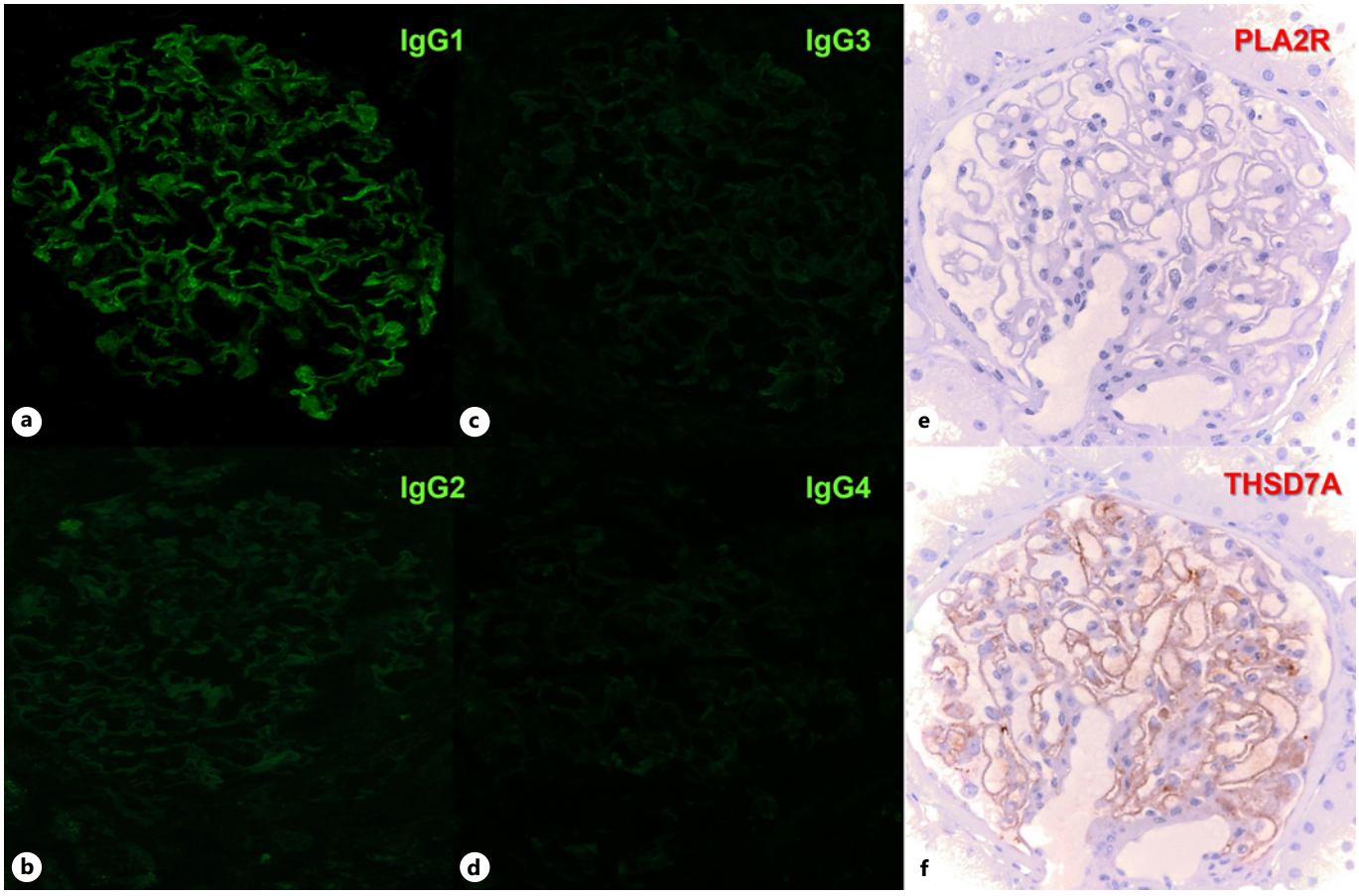

Fig. 4. A representative case of MN with global MSDs showing IgG1 predominance by IF and dual PLA2R and THSD7A negativity by immunohistochemistry. **a** IgG1. **b** IgG2. **c** IgG3. **d** IgG4. Immunohistochemistry shows that the capillary wall deposits are negative for both PLA2R (**e**) and THSD7A (**f**). There is weak podocyte cytoplasmic staining for THSD7A (**f**) but no significant capillary wall staining in the distribution of the subepithelial deposits. All images at ×400 magnification.

possibility of different pathogenic mechanisms involving the formation of microspherular and typical electron-dense deposits.

In contrast, none of the segmental MSD cases had any mesangial deposits. Only 1 of the 5 patients had a potential secondary cause (SLE), although a previous biopsy 5 years prior showed no evidence of LN and the repeat biopsy revealed MN with <20% MSD and features that were deemed inconsistent with LN.

The target antigens PLA2R and THSD7A are present in 70% and 3–5% of patients with primary MN, respectively [27]. Although several new target antigens have since been discovered, in current renal pathology practice, MN that are PLA2R or THSD7A positive are considered most likely primary, while negative staining for these antigens could be toward a secondary etiology. We performed IHC with the two available antibodies in our laboratory, PLA2R and THSD7A. In the global MSD group, all 13 assayble biopsies were negative for PLA2R, and 12 of 13 were negative for THSD7A, with one THSD7A-positive case (patient 9). These findings suggest that global MSD is associated with secondary MN. With regards to the single-positive patient, THSD7A-positive MN is associated with a higher incidence of coincident or subsequent malignancy, which could be interpreted as a secondary factor.

As mentioned previously, approximately one-third of global MSD patients had identifiable secondary causes at the time of biopsy. Although no malignancy was identified in the THSD7A-positive case, the patient was lost to follow-up, and subsequent history was unobtainable. The only 2 PLA2R-positive biopsies in the cohort were present in the segmental MSD group (2 of 5 positive) and none were THSD7A positive, suggestive of mixed

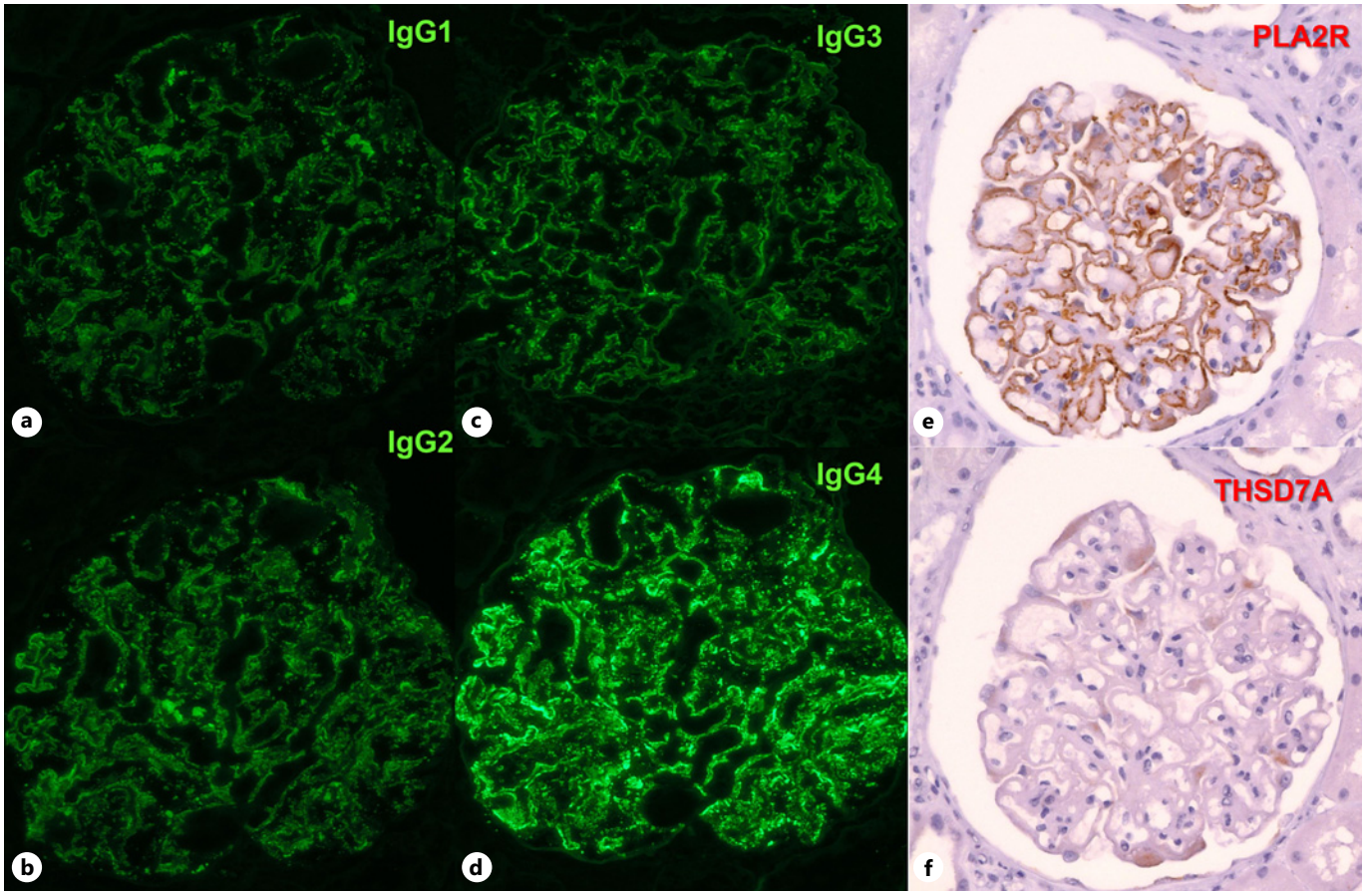

Fig. 5. A representative case of MN with segmental MSDs showing IgG4-dominant staining by IF. **a** IgG1. **b** IgG2. **c** IgG3. **d** IgG4. All at ×40 objective. Immunohistochemistry shows that the capillary wall deposits are positive for PLA2R (**e**) and are negative for THSD7A (**f**). All images at ×400 magnification.

primary and secondary MN in this group. Given the rapid rate at which new target antigens for MN are being discovered, the possibility of a novel target antigen, possibly with a non-IgG4 dominant staining phenotype, is also a consideration.

All but one of the cases for which tissue was available displayed positive IF staining for IgG along GBMs. IgG staining intensity was not weaker in the segmental MSD than in the global MSD group; in fact, the strongest IgG intensities (4+) were found only in the segmental MSD group. Furthermore, despite the very segmental nature of the MSD deposits, there was uniform staining for IgG in all GBMs (global granular) in both segmental and global MSD groups, and therefore not MSD-specific. We further performed IgG subclass staining by IF as IgG subclass patterns may have utility in distinguishing primary and secondary MN. For example, IgG4 (or IgG1 and IgG4 codominant staining) has been shown to be the predominant IgG subclass in primary MN, while IgG1 tends to be the predominant secondary MN, and IgG1, IgG2, and IgG3 are typically stronger than IgG4 in LN, with 1 of the 3 being the predominant subclass [8, 28]. In the global MSD group, all 12 biopsies with tissue available for IF showed IgG1 subclass dominance in GBM deposits, including the single THSD7A-positive biopsy, compatible with global MSDs associated with secondary MN. Nine of the 12 global MSD cases were IgG4 negative; the three remaining cases showed very weak IgG4 staining in the setting of IgG1 dominance. In contrast, in the segmental MSD group, 3 of the 5 cases had strong staining for IgG4 (≥3–4+) in a dominant pattern, with weaker or codominant staining for IgG1, IgG2 and IgG3, suggestive of mixed primary and secondary MN in this group. Of note, both PLA2R-positive cases (only present in the segmental MSD group) were also IgG4 predominant, supportive of a primary MN.

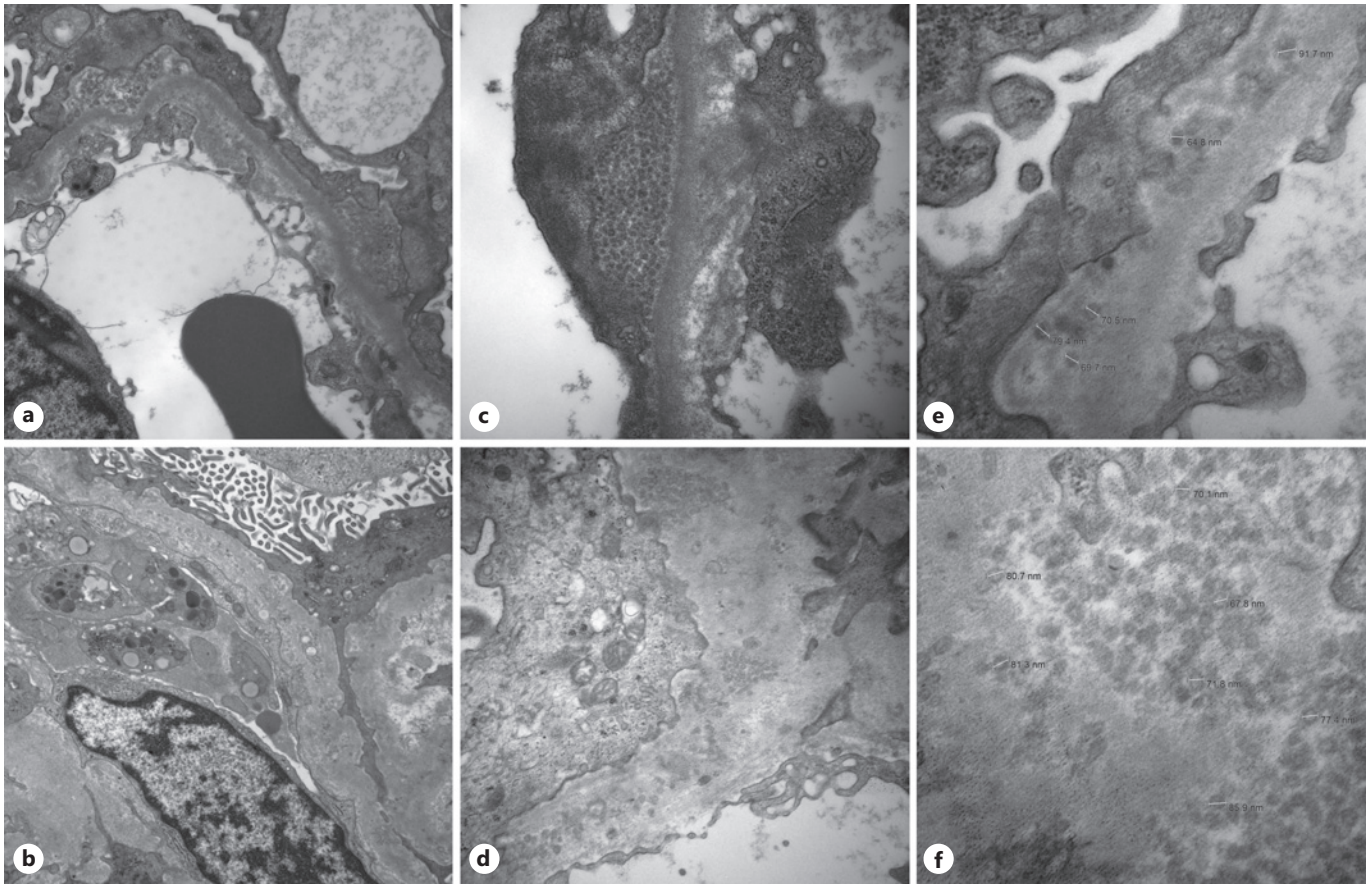

Fig. 6. Electron microscopy findings of sequential biopsies from patient 4. First biopsy shows early, Ehrenreich and Churg stage 1 subepithelial MSDs without intervening basement membrane interposition. **a** ×14,000, **b** ×36,000, **c** ×72,000 with measurements. Second biopsy 4 years later shows subepithelial and intramembranous MSDs with reabsorption changes. **d** ×14,000, **e** ×29,000, **f** ×72,000 with measurements.

Huang et al. [29] reported IgG subclass switching in primary MN from IgG1 predominance early on to IgG4 predominance later in the disease course [8, 29], and Ryan et al. [30] also reported a cohort of early primary MN that are IgG1 dominant and PLA2R negative. Exploring this possibility, we noted that both cases of early (Ehrenreich-Churg stage 1) MN in our cohort were from the global MSD group, one which had a follow-up. Patient 4 had an initial biopsy with early stage 1 membranous and IgG1 dominance. The repeat biopsy performed 4 years later showed EM progression from stage 1 to stage 4 and remained IgG1 dominant and dual negative for PLA2R and THSD7A; the lack of class switching would also seem to argue against primary MN.

While the ultrastructural properties of MSD have been characterized, the nature of these microspherular substructures remains unknown. In contrast, renal diseases with deposits with organized substructure are well established and characterized and encompass a wide range of appearances from the randomly oriented fibrils of amyloid and fibrillary glomerulonephritis to the microtubules of immunotactoid GN and cryoglobulinemic GN. While organized deposits can be associated with paraproteins, they can also be composed of non-paraprotein subunits, such as the unique properties of the mixed glomerular deposits in LN, which can range from fibrils to classic "fingerprint" substructures [31]. However, the ultrastructural appearance of MSD in our and other published cases does not resemble that of any other known organized deposits and is suggestive of a unique constituent.

One belief is that MSDs result from degradation and reabsorption of typical electron-dense deposits. In the context of MN, this would imply that MSDs should primarily be present in later stage membranous (Ehrenreich-Churg stage 3 or 4) when the deposits have been incorparated within the GBMs and undergoing resorption. However, 7 of 19 cases had evidence of MSDs early in disease

(Ehrenreich-Churg stage 1 and stage 2). Moreover, patient 4 in the global MSD group initially presented with early MN with small subepithelial MSD (Ehrenreich-Churg stage 1), and the second biopsy 4 years showed persistence of global MSD and progression to advanced MN (Ehrenreich-Churg stage 4) (shown in Fig. 6). These findings suggest that MSD may start with a unique substructure that cannot be solely explained by degradation of electron-dense immune complex deposits. Patient 13 also had repeat biopsies. The first biopsy showed moderately advanced membranous LN with significant GBM remodeling by numerous typical subepithelial and intramembranous deposits that often show rarefaction and clearing (Ehrenreich-Churg stage 3 to 4) but no MSD. However, the second biopsy 11 years later during a flare showed membranous LN with small subepithelial (Ehrenreich-Churg stage 1) MSD and healed GBM with only normal to mildly increased thickness. The near-normal GBM architecture and absence of intramembranous deposits in the second biopsy suggest disease remission with resolution of the immune complex deposits before a new LN flare-up produced the MSD.

Ultrastructural artifacts due to improper or delayed fixation, inappropriate tissue retrieval, or reprocessing from paraffin or frozen blocks can also be difficult to distinguish from organized substructure deposits by EM [32, 33]. Artifacts assuming a microspherular appearance mimicking viral particles or cross sections of microtubular structures including cryoglobulins or immunotactoids have been reported [32] and could result in misinterpretation of rare segmental MSD in MN as artifacts or clearing deposits, leading to underreporting. The microspherular structures seen in our cohort were in the absence of any other artifacts, and the persistence of the microspherular structures in sequential biopsies from patient 4 strongly suggest against this possibility.

The findings from our cohort are in concordance with those from a recently published study also examining MSD in MN [10]. Ultrastructural features of the MSD were nearly identical to those in our study, although theirs did not stratify cases based on the proportion of MSD to all deposits. Identified secondary causes in their cohort also included autoimmune diseases including SLE and 2 cases with infection (one with HCV as in our cohort). Staining for IgG subtypes revealed a mixture of patterns including IgG1 and IgG4 dominance, but interpretation was likely hindered by sample size and it is unknown if their cohort would also exhibit a similar IgG1-dominant pattern if stratified into global versus segmental MSD. All but one of their cases was negative for four different target antigen markers. The negative EXT 1/EXT 2 staining in their cohort is of particular interest, given the prevalence of underlying autoimmune disease. The conclusions from both studies indicate that MSD seem to be more frequently associated with secondary MN, specifically in the context of autoimmune disease.

This study has limitations due to the small sample size and difficulty in obtaining complete clinical information. As the majority were old cases, obtaining clinical follow-up was not possible as many of the patients were lost to follow-up. Similarly, information such as PLA2R serologic status was unavailable or simply never ordered. Additional IHC for newer antigens implicated in MN such as EXT 1/EXT 2 and NELL1 were not performed, due to the technical difficulties with likely epitope destruction from fixation in alcoholic Bouin's solution. Attempts to optimize staining in frozen and formalin-fixed tissue are underway.

Our findings suggest that MN with global MSD is associated with IgG1 subclass predominance and negative PLA2R and THSD7A staining, and therefore suggestive of secondary MN. MN with segmental MSD has mixed staining patterns for IgG subclasses and PLA2R, and may be primary or secondary. The nature and composition of MSD remain elusive, and future studies with laser microdissection mass spectrometry or immunoelectron microscopy are required to further characterize these substructures.

Statement of Ethics

This study protocol was reviewed, the need for written informed consent was waived, and the study was approved by Institutional Review Board at Cedars-Sinai Medical Center, approval number STUDY00001348.

Conflict of Interest Statement

The authors have no conflict of interest to declare.

Funding Sources

No funds were received for this study.

Author Contributions

Dr. Kevin Yi Mi Ren and Dr. Jean Hou both contributed equally to the preparation, writing, and editing of this manuscript.

Data Availability Statement

All data generated or analyzed during this study are included in this article. Further inquiries can be directed to the corresponding author.

References

1 Ronco P, Beck L, Debiec H, Fervenza FC, Hou FF, Jha V, et al. Membranous nephropathy. Nat Rev Dis Primers. 2021;7(1):69.
2 Ronco P, Debiec H. Pathophysiological advances in membranous nephropathy: time for a shift in patient's care. Lancet. 2015;385(9981):1983–92.
3 Beck LH Jr, Bonegio RG, Lambeau G, Beck DM, Powell DW, Cummins TD, et al. M-type phospholipase A2 receptor as target antigen in idiopathic membranous nephropathy. N Engl J Med. 2009;361(1):11–21.
4 Sethi S, Madden BJ, Debiec H, Charlesworth MC, Gross L, Ravindran A, et al. Exostosin 1/exostosin 2–associated membranous nephropathy. J Am Soc Nephrol. 2019;30(6):1123–36.
5 Caza TN, Hassen SI, Dvanajscak Z, Kuperman M, Edmondson R, Herzog C, et al. NELL1 is a target antigen in malignancy-associated membranous nephropathy. Kidney Int. 2021;99(4):967–76.
6 Reinhard L, Machalitza M, Wiech T, Gröne HJ, Lasse M, Rinschen M, et al. Netrin G1 is a novel target antigen in primary membranous nephropathy. J Am Soc Nephrol. 2022;33(10):1823–31.
7 Bobart SA, Tehranian S, Sethi S, Alexander MP, Nasr SH, Moura Marta C, et al. A target antigen-based approach to the classification of membranous nephropathy. Mayo Clin Proc. 2021;96(3):577–91.
8 Markowitz GS, D'Agati VD. Membranous glomerulonephritis. In: Jennette JC, Silva FG, Olson JL, D'Agati VD, editors. Heptinstall's pathology of the kidney. 7th ed. Philadelphia (PA): Wolters Kluver; 2015. Vol. 1; p. 255–99.
9 Kowalewska J, Smith KD, Hudkins KL, Chang A, Fogo AB, Houghton D, et al. Membranous glomerulopathy with spherules: an uncommon variant with obscure pathogenesis. Am J Kidney Dis. 2006;47(6):983–92.
10 Choung HYG, Jean-Gilles J, Goldman B. Subepithelial deposits with microspherular structures in membranous glomerulonephritis. Ultrastruct Pathol. 2022;46(4):377–87.
11 Dales S, Wallace AC. Nuclear pore complexes deposited in the glomerular basement membrane are associated with autoantibodies in a case of membranous nephritis. J Immunol. 1985;134(3):1588–93.
12 Mandal AK, Mask DR, Nordquist J, Chrysant KS, Lindeman RD. Membranous glomerulonephritis: virus-like inclusions in glomerular basement membrane. Ann Intern Med. 1974;80(4):554–5.
13 Joh K, Taguchi T, Shigematsu H, Kobayashi Y, Sato H, Nishi S, et al. Proposal of podocytic infolding glomerulopathy as a new disease entity: a review of 25 cases from nationwide research in Japan. Clin Exp Nephrol. 2008;12(6):421–31.
14 Zhang T, Sun W, Xue J, Chen J, Jiang Q, Mou L, et al. Podocytic infolding glomerulopathy: two new cases with connective tissue disease and literature review. Clin Rheumatol. 2019;38(5):1521–8.
15 Sato M, Kogure T, Kanemitsu M. A case of systemic lupus erythematosus showing invagination of the podocyte into the glomerular basement membrane: an electron microscopic observation of a repeated-renal biopsy. Clin Exp Nephrol. 2008;12(6):455–61.
16 Jones CA, McQuillan GM, Kusek JW, Eberhardt MS, Herman WH, Coresh J, et al. Serum creatinine levels in the US population: third national health and nutrition examination survey. Am J Kidney Dis. 1998;32(6):992–9.
17 Churg J, Ehrenreich T. Membranous nephropathy. Perspect Nephrol Hypertens. 1973;(1 Pt 1):443–8.
18 Bariety J, Callard P. Striated membranous structures in renal glomerular tufts. An electron microscopy study of 340 human renal biopsies. Lab Invest. 1975;32(5):636–41.
19 Burkholder PM, Hyman LR, Barber TA. Extracellular clusters of spherical microparticles in glomeruli in human renal glomerular diseases. Lab Invest. 1973;28(4):415–25.
20 Nazneen A, Nakashima Y, Zha Y, Le VT, Taguchi T, Nishioka K, et al. Unusual glomerulopathy with atypical thickening of the glomerular basement membrane and intramembranous microparticles. Clin Exp Nephrol. 2008;12(6):501–3.
21 Jinguji Y, Nukui I, Wakasugi M, Yamashita H. Two cases of systemic lupus erythematosus complicated by hydronephrosis and unique small structures observed in the glomerular basement membrane. Clin Exp Nephrol. 2008;12(6):467–74.
22 Fujigaki Y, Muranaka Y, Sakakima M, Ohta I, Sakao Y, Fujikura T, et al. Analysis of intra-GBM microstructures in a SLE case with glomerulopathy associated with podocytic infolding. Clin Exp Nephrol. 2008;12(6):432–9.
23 Yamada S, Masutani K, Katafuchi R, Fujigaki Y, Muranaka Y, Tsuruya K, et al. Focal segmental glomerulosclerosis with intramembranous vesicle-like microstructures and podocytic infolding lesion. Clin Exp Nephrol. 2008;12(6):509–12.
24 Nishi S, Imai N, Saito T, Ueno M, Arakawa M, Oota T, et al. A nephropathy presenting the microparticles in the glomerular basement membrane in a patient of hepatitis B viral infection. Clin Exp Nephrol. 2008;12(6):518–21.
25 Ting JA, Hung W, McRae SA, Barbour SJ, Copland M, Riazy M. Podocyte infolding glomerulopathy, first case report from north America. Can J Kidney Health Dis. 2021;8:20543581211048357.
26 Moroni G, Ponticelli C. Secondary membranous nephropathy. A narrative review. Front Med. 2020;7:611317.
27 Beck LH Jr. PLA2R and THSD7A: disparate paths to the same disease? J Am Soc Nephrol. 2017;28(9):2579–89.
28 Haas M. IgG subclass deposits in glomeruli of lupus and nonlupus membranous nephropathies. Am J Kidney Dis. 1994;23(3):358–64.
29 Huang CC, Lehman A, Albawardi A, Satoskar A, Brodsky S, Nadasdy G, et al. IgG subclass staining in renal biopsies with membranous glomerulonephritis indicates subclass switch during disease progression. Mod Pathol. 2013;26(6):799–805.
30 Ryan MS, Satoskar AA, Nadasdy GM, Brodsky SV, Hemminger JA, Nadasdy T. Phospholipase A2 receptor staining is absent in many kidney biopsies with early-stage membranous glomerulonephritis. Kidney Int. 2016;89(6):1402–3.
31 Hvala A, Kobenter T, Ferluga D. Fingerprint and other organised deposits in lupus nephritis. Wien Klin Wochenschr. 2000;112(15–16):711–5.
32 Iskandar SS, Herrera GA. Glomerular diseases with organized deposits. In: Jennette JC, Silva FG, Olson JL, D'Agati VD, editors. Heptinstall's pathology of the kidney. 7th ed. Philadelphia (PA): Wolters Kluver; 2015. Vol. 2; p. 1015–37.
33 Nakajima M, Hewitson TD, Mathews DC, Kincaid-Smith P. Localisation of complement components in association with glomerular extracellular particles in various renal diseases. Virchows Arch A Pathol Anat Histopathol. 1991;419(4):267–72.